

Generation of Multiple Sharp Fano Resonances based on a Silicon Nanobeam-Microring Resonator

Ruihuan Zhang, Yu He, Yong Zhang and Yikai Su

State Key Lab of Advanced Optical Communication Systems and Networks, Department of Electronic Engineering, Shanghai Jiao Tong University, Shanghai 200240, China
E-mail: yikaisu@sjtu.edu.cn

Abstract: A silicon nanobeam-microring resonator is experimentally demonstrated to generate periodic multiple sharp Fano resonances with an FSR of 8.44 nm. The extinction ratios of the Fano resonances are higher than 11 dB. © 2021 The Authors

1. Introduction

Fano resonance in silicon photonics has attracted considerable research interest in the past decades due to its advantages of high sensitivity in sensing and modulation applications, by leveraging the sharp asymmetric filter shape [1]. Various structures have been proposed to achieve Fano resonances, such as resonant cavities [2], Bragg gratings [3], plasmonic metamaterials [4], nanoantennas [5], and etc.. A few attempts have been made to achieve multiple Fano-resonances to enable multi-channel applications.

In this work, we propose and experimentally demonstrate the generation of multiple sharp Fano resonances based on a silicon photonic crystal nanobeam-microring resonator (PCN-MRR). The device can achieve multiple Fano resonances with an 8.44-nm free spectral range (FSR) in a wavelength range of 50.64 nm. The extinction ratios (ERs) of all the Fano resonances are higher than 11 dB.

2. Device design and simulations

Figure 1(a) and (b) show the schematic diagrams of the device. Two PCNs are embedded in the straight waveguides of the racetrack MRR, served as the reflectors. Each PCN consists of an array of 24 etched circular holes to form a Fabry-Perot (F-P) reflector, which is symmetric with respect to its center. On each side of the cavity, there are 5 holes that are adiabatically tapered from $d = 202$ nm to $d = 260$ nm to realize the phase matching between the waveguide mode and the Bloch mode, thus minimizing the scattering loss of light in the cavity. The following 7 identical holes act as the reflector mirrors. The MRR is designed with a single racetrack ring wrapped with two bend waveguides to enable sufficient coupling and a compact footprint simultaneously.

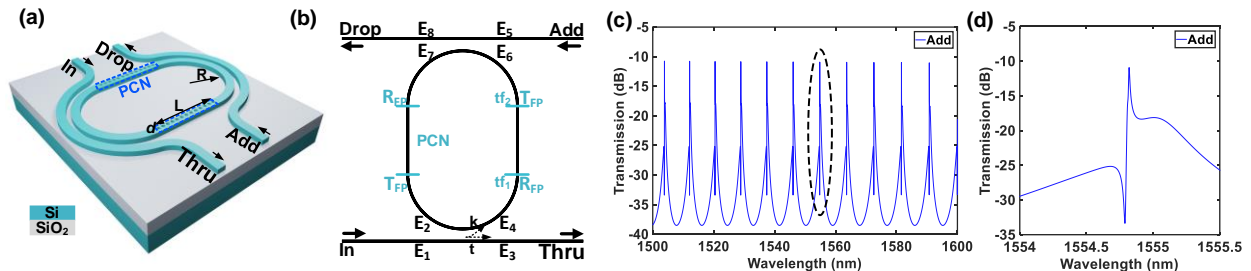


Fig. 1. (a) and (b) Schematic diagrams of the PCN-MRR resonator. (c) Simulated transmission spectra of the add port. (d) The zoomed-in figure of the black-dotted areas in (c).

We simulate the transmission spectra of the proposed structure by using the transfer matrix method, the amplitudes of the optical signals at different ports can be written as [6]:

$$\begin{bmatrix} E_4 \\ E_3 \end{bmatrix} = \begin{bmatrix} t_1 & jk_1 \\ jk_1 & t_1 \end{bmatrix} \begin{bmatrix} E_2 \\ E_1 \end{bmatrix}, \quad \begin{bmatrix} E_8 \\ E_7 \end{bmatrix} = \begin{bmatrix} t_2 & jk_2 \\ jk_2 & t_2 \end{bmatrix} \begin{bmatrix} E_5 \\ E_6 \end{bmatrix}, \quad (1)$$

where E_1, E_2, E_5, E_6 are the amplitudes of the signals at input ports for the two coupling regions, E_3, E_4, E_7, E_8 are the amplitudes of the light at output ports, t_1, t_2 are the transmission coefficients, and k_1, k_2 are the coupling coefficients. It can be obtained that $t_1^2 + k_1^2 = 1$, and $t_2^2 + k_2^2 = 1$ without considering the transmission losses.

In addition, the reflection and transmission light in the F-P reflector can be calculated as [7]:

$$R_{FP} = \frac{rf_1 - rf_2 e^{j2\phi}}{1 - rf_1 rf_2 e^{j2\phi}}, \quad T_{FP} = \frac{-tf_1 tf_2 e^{j\phi}}{1 - rf_1 rf_2 e^{j2\phi}}, \quad (2)$$

respectively, where rf_1 , rf_2 are the reflection coefficients of the reflectors, tf_1 , tf_2 are the transmission coefficients of the reflectors, $\phi = \beta L$ is the phase delay of the light, β is the propagation constant, and L is the length of the reflector. In the case of lossless condition, it can be obtained that $tf_1^2 + rf_1^2 = 1$, and $tf_2^2 + rf_2^2 = 1$.

At the steady-state, all the amplitudes are self-consistently correlated by coupling coefficients, reflection coefficients, transmission coefficients and propagation delays. Contra-directional coupling happens between the reflection induced by the F-P reflector and the traveling wave in the ring. By tuning the reflection coefficients of the F-P reflector, transmission spectra of multiple Fano resonances can be obtained at the add port of the MRR, which are shown in Fig. 1(c) and (d).

3. Fabrication and experimental results

The PCN-MRR resonator was fabricated on a silicon-on-insulator (SOI) wafer with a 220-nm top silicon layer [8]. The waveguides and the PCNs were fully etched, while the grating couplers to couple the light in and out of the device were shallowly etched with a depth of 70 nm. The device was fabricated by using E-beam lithography (EBL) (Vistec EBPG 5200+) and inductively coupled plasma (ICP) etching (SPTS DRIE-I). Figure 2(a) shows the scanning electron microscope (SEM) image of the fabricated device structure. The footprint of the device is $31 \mu\text{m} \times 26 \mu\text{m}$. The yellow-dotted areas are the PCN-based F-P reflectors. The performance of the fabricated device was characterized by using a tunable laser (Keysight 81960), and an optical power meter. Figure 2(b) shows the measured transmission spectra at the add port of the device. In the wavelength range of 1529.05 nm to 1579.69 nm, seven sharp Fano resonances are generated with an FSR of 8.44 nm. All the ERs of the Fano resonances are higher than 11 dB, where the ER is defined from the peak to the notch of an asymmetric resonance. It is noticed that certain fluctuations exist in the transmission spectra, which are attributed to the random radiation losses in the device induced by imperfect fabrication process. Figure 2(c) shows the zoom-in picture of the Fano resonance at the wavelength of 1537.23 nm, where the ER is ~ 17 dB from the peak to the dip, with a slope rate (SR) of 115 dB/nm.

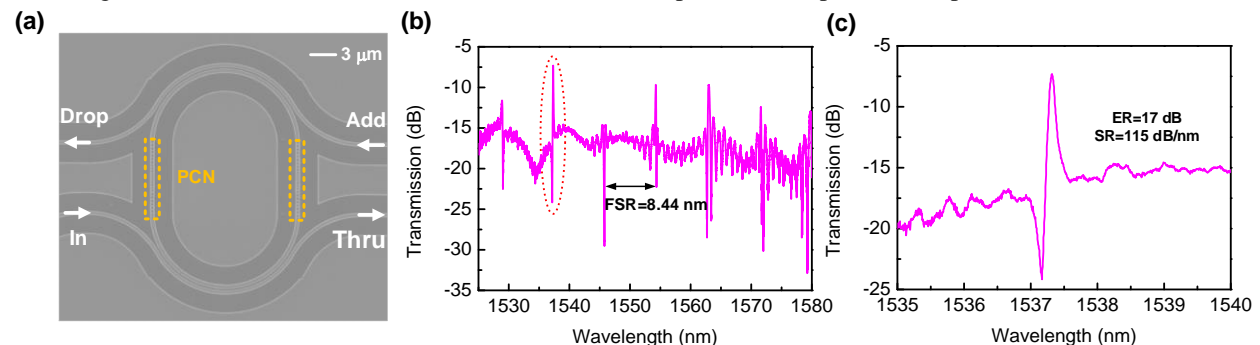


Fig. 2. (a) SEM image of the PCN-MRR based resonator. (b) Measured transmission spectra at the add port. (c) The zoomed-in figure of the red-dotted areas in (b).

4. Conclusion

We demonstrate a compact PCN-MRR resonator to generate multiple sharp Fano resonances. The experimental results show that seven sharp Fano resonances are generated with an 8.44-nm FSR in a wavelength range of 50.64 nm. The ERs of the Fano resonances are higher than 11 dB. The footprint of the device is $31 \mu\text{m} \times 26 \mu\text{m}$.

5. References

- [1] M. F. Limonov et al., "Fano resonances in photonics," *Nature Photonics*, **11**(9), 543-554 (2017).
- [2] Z. Zhang et al., "The switchable EIT-like and Fano resonances in microring-Bragg grating based coupling resonant system," *Proc. CLEO SM1N.8* (2017).
- [3] M. V. Rybin et al., "Bragg scattering induces Fano resonance in photonic crystals," *PHOTONICS AND NANOSTRUCTURES*, **8**(2), 86-93 (2010).
- [4] Z. Meng et al., "Realizing prominent Fano resonances in metal-insulator-metal plasmonic Bragg gratings side-coupled with plasmonic nanocavities," *Plasmonics*, **13**, 2329-2336 (2018).
- [5] F. López-Tejedor et al., "Fano-like interference of plasmon resonances at a single rod-shaped nanoantenna," *New J. Phys.* **14**(2), 023035 (2012).
- [6] J. Heebner et al., "Optical Microresonators," Springer New York (2008).
- [7] N. Ismail et al., "Fabry-Perot resonator: spectral line shapes, generic and related Airy distributions, linewidths, finesses, and performance at low or frequency-dependent reflectivity," *Opt. Express*, **24**(15), 16366-16389 (2016).
- [8] Y. Su et al., "Silicon photonic platform for passive waveguide devices: materials, fabrication, and applications," *Adv. Mater. Technol.*, 1901153, 1-19 (2020).